

An abrupt drop in Northern Hemisphere sea surface temperature around 1970

David W. J. Thompson¹, John M. Wallace², John J. Kennedy³ & Phil D. Jones⁴

The twentieth-century trend in global-mean surface temperature was not monotonic: temperatures rose from the start of the century to the 1940s, fell slightly during the middle part of the century, and rose rapidly from the mid-1970s onwards¹. The warming-cooling-warming pattern of twentieth-century temperatures is typically interpreted as the superposition of long-term warming due to increasing greenhouse gases and either cooling due to a mid-twentieth century increase of sulphate aerosols in the troposphere²⁻⁴, or changes in the climate of the world's oceans that evolve over decades (oscillatory multidecadal variability)^{2,5}. Loadings of sulphate aerosol in the troposphere are thought to have had a particularly important role in the differences in temperature trends between the Northern and Southern hemispheres during the decades following the Second World War²⁻⁴. Here we show that the hemispheric differences in temperature trends in the middle of the twentieth century stem largely from a rapid drop in Northern Hemisphere sea surface temperatures of about 0.3 °C between about 1968 and 1972. The timescale of the drop is shorter than that associated with either tropospheric aerosol loadings or previous characterizations of oscillatory multidecadal variability. The drop is evident in all available historical sea surface temperature data sets, is not traceable to changes in the attendant metadata, and is not linked to any known biases in surface temperature measurements. The drop is not concentrated in any discrete region of the Northern Hemisphere oceans, but its amplitude is largest over the northern North Atlantic.

Significant events in the hemispheric or global-mean surface temperature records are obscured by year-to-year variability induced by a variety of physical processes, notably: changes in the Northern Hemisphere high-latitude wintertime atmospheric circulation that modulate the strength of the advection of warm, marine air masses over the cold continents; the El Niño Southern Oscillation (ENSO) cycle, which modulates the exchange of heat between the atmosphere and ocean; and/or volcanic eruptions, which inject long-lived, reflective sulphate aerosols into the stratosphere. Two recent analyses of global-mean surface temperatures^{6,7} describe a method of suppressing the effects of these three processes from the surface temperature record to reveal or highlight significant events without reducing the time resolution of the data, thereby preserving the statistical degrees of freedom in the raw time series.

Figure 1a shows the results of applying this methodology to remove the effects of the three processes listed above from the time series of global-mean surface temperature (ref. 7; Supplementary Information). The residual global-mean temperature time series (Fig. 1a, bottom) indicates that the apparent hiatus in global warming during the mid-twentieth century is mainly the result of two distinct events: an abrupt drop in temperatures in 1945 and a roughly decade-long dip in global-mean temperatures that began in the 1960s. The drop in 1945 was identified in ref. 6 and is linked to biases in the sea surface temperature (SST) data. The purpose of this study is to highlight prominent but previously overlooked aspects of the nature of the cooling event that began in the 1960s.

The upper two time series in Fig. 1b show SSTs averaged over the Northern and Southern hemispheres. Northern Hemisphere SST exhibited little upward trend between about 1945 and 1980, but then warmed quite rapidly during the 1980s and 1990s. In contrast, Southern Hemisphere SST rose much more steadily throughout the second half of the twentieth century. That the mid-twentieth-century warming was more pronounced in the Southern Hemisphere than in the Northern Hemisphere has been widely noted¹ and is consistent with hemispheric differences in the history of tropospheric sulphate aerosol loadings: anthropogenic emissions of sulphate aerosols increased most rapidly in the mid-twentieth century over North America, Europe and Asia, and hence the rate of aerosol-induced cooling—which counters greenhouse warming—should have been more pronounced over the Northern Hemisphere than over the Southern Hemisphere²⁻⁴. However, when the Southern Hemisphere-mean SST time series is subtracted from the Northern Hemisphere-mean SST time series (NH – SH SST; Fig. 1b, bottom), it becomes apparent that Northern Hemisphere SST did not cool relative to Southern Hemisphere SST over a period of decades, as would be expected if the cooling were in response to a gradual build-up of sulphate aerosol loadings. Rather, Northern Hemisphere SST dropped sharply relative to Southern Hemisphere SST between 1968 and 1972, and NH – SH SST stayed low relative to pre-1970 values throughout the remainder of the twentieth century (Fig. 1b, bottom time series).

The sudden drop in NH – SH SST centred around 1970 stems almost entirely from the Northern Hemisphere. Figure 1c shows the data from Fig. 1b adjusted to suppress the variance associated with the ENSO cycle and the response to volcanic eruptions, as described in the Supplementary Information and ref. 7. The upper two time series in Fig. 1c show the discontinuity in the SST data in 1945, which is apparent in both hemispheres. But they also show a second drop centred around 1970, which is apparent only in the Northern Hemisphere. This latter drop is comparable in amplitude to the drop due to instrument biases in 1945, and it seems to be responsible for most of the sudden drop in NH – SH SST shown in the bottom time series of Fig. 1b. The NH – SH SST time series at the bottom of Fig. 1c is nearly identical to the unadjusted version shown at the bottom of Fig. 1b, because the signatures of ENSO and volcanic eruptions are effectively removed from the unadjusted data when the hemispheric means are subtracted from one another.

The prevailing view of twentieth-century SST variability is that Northern Hemisphere SST decreased smoothly in the decades following the Second World War, and/or oscillated continuously on multi-decadal timescales throughout the twentieth century^{5,8-13}. This view is derived from analyses based on either spectrally filtered^{8,9} or low-pass filtered^{5,10-13} versions of the data, which are incapable of revealing sudden changes in SSTs owing to the method of their construction. The monthly-resolution residual time series in Fig. 1c give a different picture of observed mid-century SST variability. Northern Hemisphere SSTs did not oscillate continuously on multi-decadal timescales, but rose steadily throughout the twentieth century apart from two discrete

¹Department of Atmospheric Science, Colorado State University, Fort Collins, Colorado 80523, USA. ²Department of Atmospheric Sciences, University of Washington, Seattle, Washington 98195-1640, USA. ³Met Office Hadley Centre, Met Office, Exeter EX1 3PB, UK. ⁴Climatic Research Unit, University of East Anglia, Norwich NR4 7TJ, UK.

events: the drops in 1945 and around 1970. The suddenness of the drop around 1970 becomes apparent when we adjust the Northern Hemisphere data to suppress the effects of ENSO and volcanic eruptions without reducing the time resolution of the data (Fig. 1c, top), or when we subtract the monthly-resolution Northern Hemisphere SST and Southern Hemisphere SST from one another (Figs 1b and c, bottom). The suddenness of the drop in Northern Hemisphere SSTs is reminiscent of ‘abrupt climate change’, such as has been inferred from the palaeoclimate record¹⁴, but is inevitably obscured in analyses of twentieth century decadal variability based on low-pass filtered versions of the SST data. A similar drop is evident in the fourth empirical orthogonal function of the global SST field¹⁵, but such high-order

empirical orthogonal functions are difficult to reproduce and to interpret physically owing to the orthogonality constraints placed on them.

Unlike the discontinuity in global-mean SSTs at 1945 (ref. 6) the drop in NH – SH SST around 1970 is not linked to any known biases in the SST data. As shown in Fig. 2a, the drop is evident in the uncorrected gridded summaries calculated from the International Comprehensive Ocean-Atmosphere Data Set version 2.4 (ICOADS2.4; ref. 16), and also the recently available ICOADS update (ICOADS2.5; ref. 17). It is present in all historical SST products derived primarily from ICOADS measurements, including the Met Office Hadley Centre’s SST data set (HadSST2), the Extended Reconstruction SST (ERSSTv3b) product developed at the US National Oceanic and Atmospheric

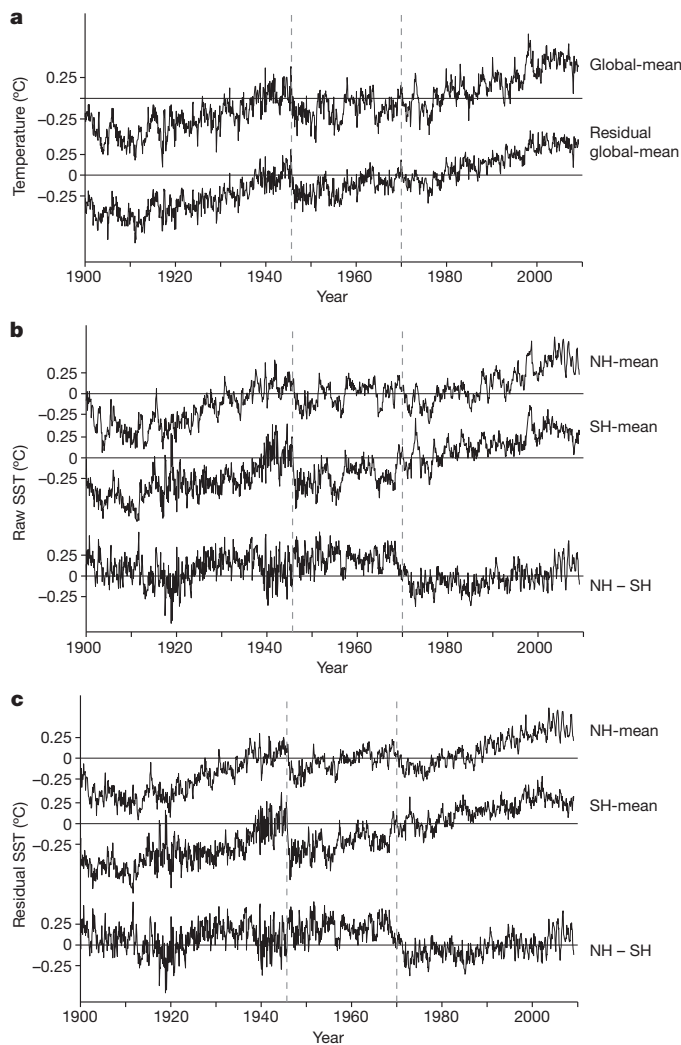


Figure 1 | Global- and hemispheric-mean surface temperatures since 1900. **a**, The raw (top) and residual (bottom) global-mean temperature time series (land + ocean) from the HadCRUT3 data set. The residual time series has been adjusted to suppress the effects of ENSO, temperature advection, and volcanic eruptions, as described in the Supplementary Information and ref. 7. The data are described in the Methods Summary. **b**, Northern Hemisphere mean SSTs (top); Southern Hemisphere mean SSTs (middle); NH minus SH (NH – SH) SSTs (bottom). Results are based on data from the HadSST2 data set. NH, Northern Hemisphere; SH, Southern Hemisphere. **c**, As in **b**, but for residual SST time series that have been adjusted to suppress effects of ENSO and volcanic eruptions, as described in the Supplementary Information and ref. 7. The full decomposition of the Northern Hemisphere and Southern Hemisphere SST time series is shown in the Supplementary Information. The dashed vertical lines in all figures correspond to the months September 1945 and January 1970.

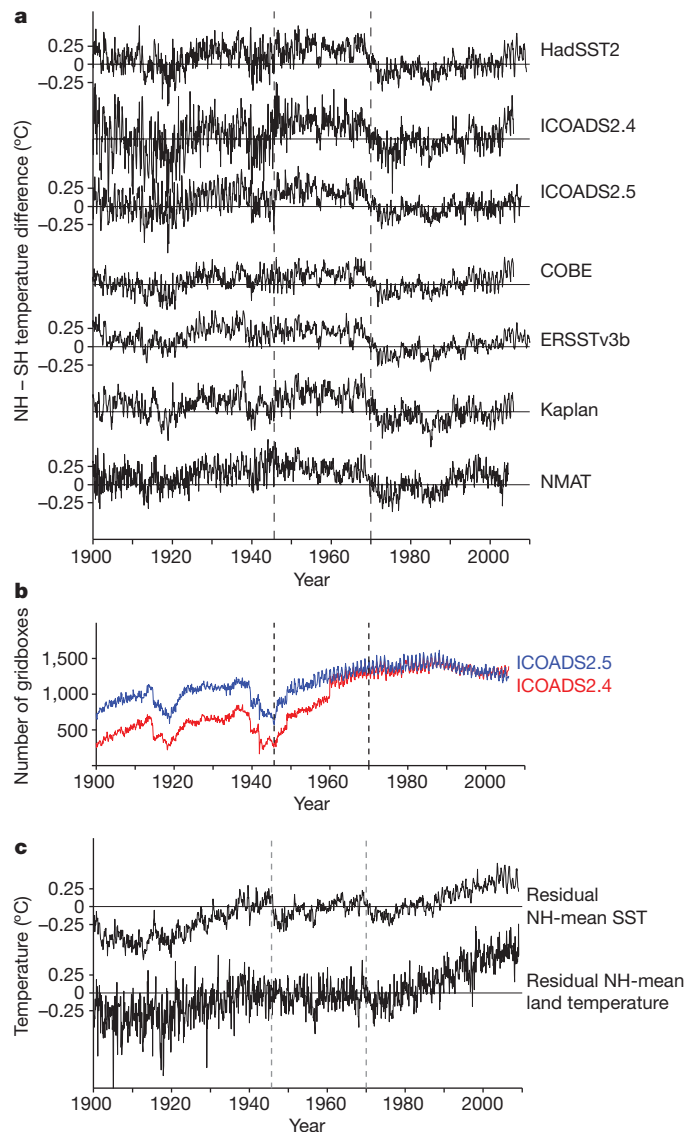


Figure 2 | Establishing the robustness of the drop in NH – SH SSTs around 1970. **a**, The NH – SH SST time series calculated for the HadSST2 data (duplicated from Fig. 1b) plotted alongside the NH – SH time series calculated for two versions of ICOADS, the COBE, ERSSTv3b and Kaplan SST data sets, and night-time marine air temperature data. See text and Methods Summary for details of the data sources. **b**, The number of 5° × 5° grid boxes populated with data re-gridded from ICOADS2.4 (red) and ICOADS2.5 (blue). Note that the number of observations does not change noticeably around the drop in 1970. **c**, The residual Northern Hemisphere SST time series duplicated from Fig. 1c (top) and the residual land temperature time series from the CRUTEM3 data set (bottom). The residual land time series has been adjusted to suppress the effects of ENSO, temperature advection, and volcanic eruptions, as described in the Supplementary Information and ref. 7.

Administration's National Climatic Data Center, the Kaplan Extended SST data set developed at the Lamont–Doherty Earth Observatory, and the Centennial *in situ* Observation-Based Estimates (COBE) SST product developed at the Japanese Meteorological Agency (Fig. 2a; see Methods Summary for data sources). The drop is not tied to any apparent changes in the volume of available observations (Fig. 2b) or any known changes in SST measurement techniques recorded in the meta-data (Supplementary Information), and it is not unique to observations made by ships from a single country of origin (Supplementary Information). A drop around the same time is also evident in measurements of night-time marine air temperature data, which are processed very differently from the SST data (Fig. 2a bottom). And a concurrent drop is evident in the fully independent Northern Hemisphere land temperature data, particularly when those data have been adjusted to suppress the effects of variations in the high-latitude atmospheric circulation, ENSO, and volcanic eruptions (Fig. 2c, bottom; see Supplementary Information for details of the adjustment). The rapid drop in NH – SH SSTs around 1970 seems to be a real and robust aspect of twentieth-century climate variability.

The timescale of the drop is important, because it is considerably shorter than that typically associated with either tropospheric aerosol forcing^{2–4} or oscillatory multidecadal SST variability^{8–13}. The horizontal structure of the drop is also of interest, because it indicates that the drop might reflect atmosphere–ocean interaction in the dynamically active northern North Atlantic. We investigated the structure of the drop by regressing SST data that have been weighted by a triangular function centred about 1970, with end points in 1940 and 2000, onto a time series of the drop formed by fitting a polynomial function to the

NH – SH SST time series (see Supplementary Information for details of the regression). The resulting regression map reveals that the drop is reflected throughout much of the world's ocean, but has its largest amplitude over the northern North Atlantic (Fig. 3a). The spatial concentration of the drop can also be seen in residual SST time series calculated for select Northern Hemisphere ocean areas; it is evident in area averages for the entire North Atlantic and North Pacific Oceans, but has its largest amplitude in data averaged over the northern North Atlantic, above 50° N (Fig. 3b). This region is marked by large exchanges of heat between the ocean and atmosphere that are considered capable of influencing hemispheric-mean temperature^{5,18}. The timing of the drop corresponds closely to a rapid freshening of the northern North Atlantic in the late 1960s/early 1970s (the 'great salinity anomaly'¹⁹).

The spatial and temporal structures of the drop in NH – SH sea-surface temperatures suggest that the hemispheric differences in surface temperature trends during the mid-twentieth century derive not from hemispheric asymmetries in tropospheric aerosol loadings^{2–4} or oscillatory decadal variability in the ocean^{8–13}. Rather, the hemispheric differences seem to derive in large part from a discrete cooling event in the Northern Hemisphere oceans that was not geographically localized, but had its largest amplitude over the northern North Atlantic.

METHODS SUMMARY

All data used in the analyses are available through the online Supplementary Information. We obtained the primary data sets from the Climatic Research Unit (<http://www.cru.uea.ac.uk>). They are: the CRUTEM3 monthly-mean land surface data set²⁰; the HadSST2 SST data set²¹; and the HadCRUT3 combined land and sea surface temperature data set²⁰.

The ICOADS data are described in refs 16 and 17, and we obtained the gridded summaries of ICOADS2.4 from <http://ghrsst.nodc.noaa.gov/intercomp.html>. The ICOADS2.5 data are described in ref. 17 and we obtained the gridded summaries (the 'standard' product) and climatological means (based on the latest 'enhanced' product) from <http://www.esrl.noaa.gov/psd/data/gridded/data.coads.2deg.html> and <http://www.esrl.noaa.gov/psd/data/gridded/data.coads.ltm.html>, respectively, and re-gridded them onto a five-degree grid. The World Meteorological Organization Publication No. 47 metadata files (which are also preserved in the online Supplementary Information) are described in ref. 22.

We obtained the COBE SST analysis²³ and the Kaplan SST data set²⁴ from <http://ghrsst.nodc.noaa.gov/intercomp.html>. We obtained the ERSSTv3b data²⁵ from <http://www.ncdc.noaa.gov/oa/climate/research/sst/ersstv3.php>. The night-time marine air temperature data are from the Hadley Centre Marine Air Temperature data set (HadMAT; ref. 21).

The COBE SST analysis is based on ICOADS2.0 and additional data from the Kobe collection (later incorporated into ICOADS2.5). The ERSSTv3b data set is based on ICOADS2.4. The Kaplan SST data set is based on data from COADS (ref. 26) and the Met Office Marine Data Bank (both sources are now incorporated into ICOADS2.5).

The methodologies used to estimate the effects on area-averaged temperatures of the advection of warm, marine air masses over the cold continents, the ENSO cycle, and volcanic eruptions are based on statistical and thermodynamic models of the climate system, and are described in the Supplementary Information and in ref. 7.

Received 19 January; accepted 20 July 2010.

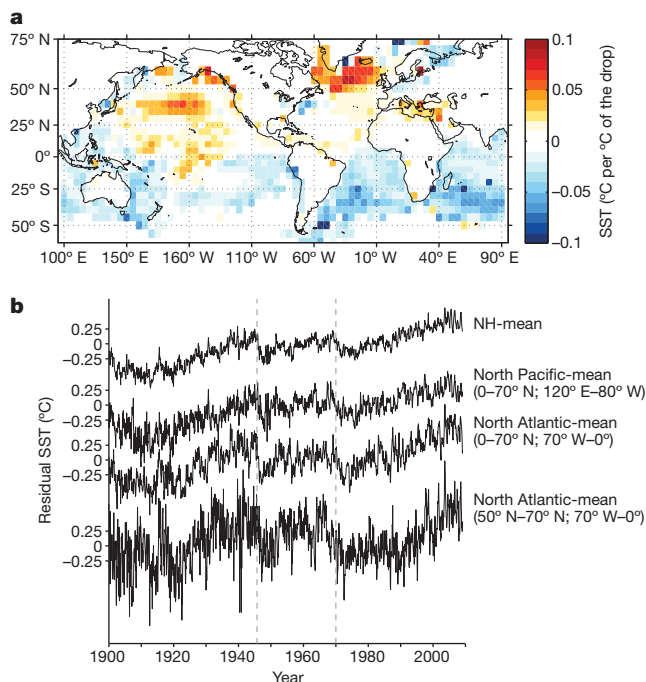


Figure 3 | Identifying the horizontal structure of the drop. **a**, The regression map formed by regressing SST data that have been weighted by a triangular function centred about 1970, with end points in 1940 and 2000, onto a time series of the drop. The time series of the drop was generated by fitting a third-order polynomial fit to the NH – SH time series from Fig. 1b for the period 1968–1972, and then extending the resulting fitted time series backwards and forwards over various time intervals centred about 1970 using fixed pre- and post-drop values for years before 1968 and after 1972. Units for regressed SST are degrees Celsius per degree in the drop around 1970. Details of the analysis and the fitted time series of the drop are included in the Supplementary Information. **b**, Residual SST time series for the regions indicated. The residual SST time series have been adjusted to suppress the effects of ENSO and volcanic eruptions, as described in the Supplementary Information and ref. 7.

1. Trenberth, K. *et al.* in *Climate Change 2007: The Physical Science Basis. Contribution of Working Group I to the Fourth Assessment Report of the Intergovernmental Panel on Climate Change* Ch. 3 (Cambridge Univ. Press, 2007).
2. Hegerl, G. *et al.* in *Climate Change 2007: The Physical Science Basis. Contribution of Working Group I to the Fourth Assessment Report of the Intergovernmental Panel on Climate Change* Ch. 9 (Cambridge Univ. Press, 2007).
3. Tett, S. F. B. *et al.* Estimation of natural and anthropogenic contributions to twentieth century temperature change. *J. Geophys. Res.* **107**, 4306 (2002).
4. Stott, P. A. *et al.* Observational constraints on past attributable warming and predictions of future global warming. *J. Clim.* **19**, 3055–3069 (2006).
5. Knight, J. R., Allan, R. J., Folland, C. K., Vellinga, M. & Mann, M. E. A signature of persistent natural thermohaline circulation cycles in observed climate. *Geophys. Res. Lett.* **32**, L20708 (2005).
6. Thompson, D. W. J., Kennedy, J. J., Wallace, J. M. & Jones, P. D. A large discontinuity in the mid-twentieth century in observed global-mean surface temperature. *Nature* **453**, 646–649 (2008).
7. Thompson, D. W. J., Wallace, J. M., Jones, P. D. & Kennedy, J. J. Identifying signatures of natural climate variability in time series of global-mean surface temperature: methodology and insights. *J. Clim.* **22**, 6120–6141 (2009).

8. Schlesinger, M. E. & Ramankutty, N. An oscillation in the global climate system of period 65–70 years. *Nature* **367**, 723–726 (1994).
9. Delworth, T. L. & Mann, M. E. Observed and simulated multidecadal variability in the Northern Hemisphere. *Clim. Dyn.* **16**, 661–676 (2000).
10. Enfield, D. B., Mestas-Nuñez, A. M. & Trimble, P. J. The Atlantic Multidecadal Oscillation and its relation to rainfall and river flows in the continental U.S. *Geophys. Res. Lett.* **28**, 2077–2080 (2001).
11. Sutton, R. T. & Hodson, D. L. R. Atlantic Ocean forcing of North American and European summer climate. *Science* **309**, 115–118 (2005).
12. Trenberth, K. E. & Shea, D. J. Atlantic hurricanes and natural variability in 2005. *Geophys. Res. Lett.* **33**, L12704 (2006).
13. Baines, P. G. & Folland, C. K. Evidence for a rapid global climate shift across the late 1960s. *J. Clim.* **20**, 2721–2744 (2007).
14. Jansen, E. *et al.* in *Climate Change 2007: The Physical Science Basis. Contribution of Working Group I to the Fourth Assessment Report of the Intergovernmental Panel on Climate Change* Ch. 6 (Cambridge Univ. Press, 2007).
15. Dima, M. & Lohmann, G. Evidence for two distinct modes of large-scale ocean circulation changes over the last century. *J. Clim.* **23**, 5–16 (2010).
16. Worley, S. J., Woodruff, S. D., Reynolds, R. W., Lubker, S. J. & Lott, N. ICOADS release 2.1 data and products. *Int. J. Climatol.* **25**, 823–842 (2005).
17. Woodruff, S. D. *et al.* ICOADS release 2.5: extensions and enhancements to the surface marine meteorological archive. *Int. J. Climatol.* doi:10.1002/joc.2103 (2010).
18. Zhang, R., Delworth, T. L. & Held, I. M. Can the Atlantic Ocean drive the observed multidecadal variability in Northern Hemisphere mean temperature? *Geophys. Res. Lett.* **34**, L02709 (2007).
19. Dickson, R. R., Meincke, J., Malmber, S. A. & Lee, A. J. The “great salinity anomaly” in the northern North Atlantic 1968–1982. *Prog. Oceanogr.* **20**, 103–151 (1988).
20. Brohan, P., Kennedy, J. J., Harris, I., Tett, S. F. B. & Jones, P. D. Uncertainty estimates in regional and global observed temperature changes: a new dataset from 1850. *J. Geophys. Res.* **111**, D12106 (2006).
21. Rayner, N. A. *et al.* Improved analyses of changes and uncertainties in marine temperature measured in situ since the mid-nineteenth century: the HadSST2 dataset. *J. Clim.* **19**, 446–469 (2006).
22. Kent, E. C., Woodruff, S. D. & Berry, D. I. WMO Publication No. 47 metadata and an assessment of observation heights in ICOADS. *J. Atmos. Ocean. Technol.* **24**, 214–234 (2007).
23. Ishii, M., Shouji, A., Sugimoto, S. & Matsumoto, T. Objective analyses of sea-surface temperature and marine meteorological variables for the 20th century using ICOADS and the Kobe Collection. *Int. J. Climatol.* **25**, 865–879 (2005).
24. Kaplan, A. *et al.* Analyses of global sea surface temperature 1856–1991. *J. Geophys. Res.* **103**, 18567–18589 (1998).
25. Smith, T. M., Reynolds, R. W., Peterson, T. C. & Lawrimore, J. Improvements to NOAA’s historical merged land–ocean surface temperature analysis (1880–2006). *J. Clim.* **21**, 2283–2296 (2008).
26. Woodruff, S. D., Slutz, R. J., Jenne, R. L. & Steurer, P. M. A comprehensive ocean–atmosphere data set. *Bull. Am. Meteorol. Soc.* **68**, 1239–1250 (1987).

Supplementary Information is linked to the online version of the paper at www.nature.com/nature.

Acknowledgements D.W.J.T. and J.M.W. are supported by the National Science Foundation Climate Dynamics Program under budget numbers ATM-0132190 and ATM-0613082 (D.W.J.T.) and ATM-0812802 (J.M.W.). J.J.K. is supported by the Joint Department of Energy and Climate Change and Defra Integrated Climate Programme: DECC/Defra (GA01101).

Author Contributions J.M.W. contributed to the text, to the analysis design, and to the physical interpretation of the results. J.J.K. contributed to the text, performed all analyses of the metadata, and provided assistance with the analyses in the main text. P.D.J. contributed to the text, provided guidance on the context of the results, and provided expertise on the data sets used in the analyses. D.W.J.T. designed and carried out the primary analyses and led the writing of the text.

Author Information Reprints and permissions information is available at www.nature.com/reprints. The authors declare no competing financial interests. Readers are welcome to comment on the online version of this article at www.nature.com/nature. Correspondence and requests for materials should be addressed to D.W.J.T. (davet@atmos.colostate.edu).